

The theory of focusing of high energy ions by bent crystals of special shape

Gennady V. Kovalev

*School of Mathematics
University of Minnesota, Minneapolis, MN 55455, USA*

Abstract

In this report we present the detail theory of the focusing in bent crystals using the statistical mechanics. The quantum mechanical effects for focusing and aberrations are not considered. The beam structure in phase space are considered and envelope near the focusing spot and intensity profile are derived.

Key words: channeling; particle beam; beam focusing; bent crystal; microbeam; nuclear microprobe;

PACS: 61.85.+; 29.27.-a; 41.75.ak; 25.43.+

1 Introduction

When a high energy particle with a momentum P are captured in a channeling motion of bent crystal, the equivalent magnetic field acting on the particle can be estimated as $\sim P/(0.3R)$, where R is a curvature radius of the bent crystal [1,2]. For the momentums $P \gtrsim 300\text{GeV}/c$ and radius $R \sim 1\text{m}$ the equivalent magnetic field can reach the values $\gtrsim 1000$ tesla. This phenomena has been extensively investigated for a beam deflection, splitting, extraction, and spin precession measurements[2,3,4]. The first experiment of the bent channeling[5] confirmed that the bent crystal could also be used for constructing a focusing element with extremely short focal length and small focal spot. Several crystal devices for focusing were suggested[6,7,8,9], but the successful experiments[10,11] were done with the crystal having a special shape drawn in Fig. 1(a). This is a regular bent crystal with the output face carved in such a way that the tangent lines to the planar channels on that face are converged to a focal point. With these conditions, the center points of the channels on the output face of the crystal constitute a cylindrical surface with diameter D , greater than curvature radii of bending, $D \geq R_{max} \geq R \geq R_{min}$. The estimations[12] show that the size of smallest focal spot is proportional to the

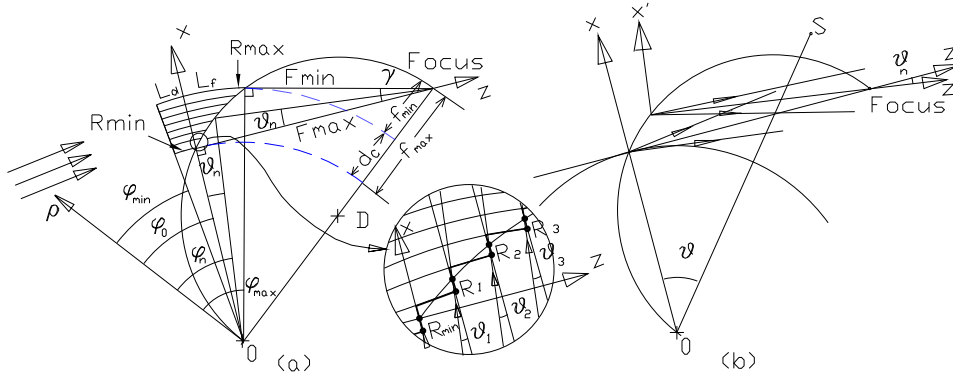


Fig. 1. Geometry of focusing crystal for high energy particles (angles, thicknesses and curvatures are exaggerated). (a) The radius-vectors R_0, R_1, \dots, R_N originated from center O designate the curvature of each plane. (b) The n -th channel ($n = 1, 2, 3 \dots N$) is located between n -th and $(n+1)$ -th planes and has a 'local' Cartesian coordinate system (x', z') with offset (x_n, z_n) and angle direction $\vartheta_n = \varphi_n - \varphi_0$ relatively to 'base' Cartesian coordinate system (x, z) of the channel 0.

square root of the crystal thickness d_c . There is also an evaluation of the intensity at the focal spot, and the crystal geometry is proposed where the focal parameters can reach the extreme values.

In this article we present the detail theory of the focusing in bent crystals using the statistical mechanics. The quantum mechanical effects for focusing and aberration are not considered here.

2 The model potential of focusing by bent crystal

We consider the classical model of channeling [13] with a continuous temperature dependent planar potential, when ions are captured into channeling trajectories and directed along the bent atomic channels. Similar considerations in bent crystals without boundary conditions were done by many authors [14,15,16,17,4] and based on the assumption that curvatures of crystalline structure are small and bent plane locally looks like flat surface. In local coordinate system the model of continuous straight planar potential [13] can be apply and describe the most important features of bent channeling [4]. If each plane has a constant curvature, it is convenient to use a polar coordinate system (ρ, φ) with a center located at the point O (see Fig. 1(a)) and direction $(\rho, \varphi = 0)$ tangent to the cylindrical surface. In such coordinate system the crystal potential for the bent channeling in Moliere's approximation [18,19,20] with a different length of the channels can be described as following

$$U_{b-c}(\rho, \varphi) = \sum_{n=0}^N U_n(\rho - R_n, \varphi), \quad (1)$$

where $R_n = R_{min} + n * d_p$ is the radius of curvature of n -th bent plane ($R_0 = R_{min}, R_N = R_{max}$), d_p is interplanar distance, $U_n(\rho - R_n, \varphi)$ is temperature-dependent continuum potential of this plane derived from the Moliere potential [21,22] for straight plane:

$$U_n(\xi, \varphi) = \begin{cases} \bar{U} \sum_{i=1}^3 \frac{\alpha_i}{\beta_i} \exp(\beta_i^2 \frac{u^2}{2a^2}) \\ (\exp(\beta_i \frac{\xi}{a}) \operatorname{erfc}(\beta_i \frac{u}{\sqrt{2a}} + \frac{\xi}{\sqrt{2u}}) \\ + \exp(-\beta_i \frac{\xi}{a}) \operatorname{erfc}(\beta_i \frac{u}{\sqrt{2a}} - \frac{\xi}{\sqrt{2u}})), \varphi_{min} < \varphi < \varphi_n, \\ 0, \varphi < \varphi_{min}, \quad \varphi > \varphi_n. \end{cases} \quad (2)$$

Here a and u are Thomas-Fermi screen radius and root-mean-square temperature displacement of crystal atoms (in Si at 293K $u = 0.075\text{\AA}$), $\alpha_i = \{.1, .55, .35\}$, $\beta_i = \{6.0; 1.2; .3\}$, $\bar{U} = \pi Z e^2 a n_p$ (n_p is a density of atoms in the plane), $\operatorname{erfc}(x)$ is the complementary error function. The angles φ_{min}, φ_n denote the enter and exit surfaces of the n th bent plane. Thus, the end cylindrical surface of the crystal lies in the range $\varphi_0 < \varphi < \varphi_{max}$. Others notations can be found in Fig. 1. Although Moliere's approximation (2) for isolated plane has a simple analytical form, it can not directly be implemented for calculation of the channeling trajectory, because the channel potential is superposed from several neighboring planes. However, if we consider an infinite crystal at fixed temperature, this superposition can be fitted by a polynomial of suitable order. The estimations can be easily received by an harmonic approximation [4], which coincides with Moliere's approximation on the crystalline planes and on centers of the channels. By involving 10 crystalline planes located far away from boundaries ($K \gg 1$), the parabolic potential can be fitted to the Moliere's approximation with the following parameters:

$$U_{max} = \sum_{n=K-4}^{K+5} U_n((K-n) * d_p, \varphi),$$

$$U_{min} = \sum_{n=K-4}^{K+5} U_n((K-n) * d_p - d_p/2, \varphi). \quad (3)$$

One can extend this model to the crystalline potential near the boundaries ignoring the fact that potential of the first several subsurface channels becomes slightly asymmetric (see Fig. 2). Outside the crystal, the potential can also be fitted by half part of parabola, for example, with a condition that on the boundary plane the potential is continuous and the parabola intersects the Moliere's potential at the value $U_{min}/2$. Because other planes give a small contribution to the surface potential, the distance of this intersection from boundary plane is very close to $d_p/2$. The resulting system of two equations,

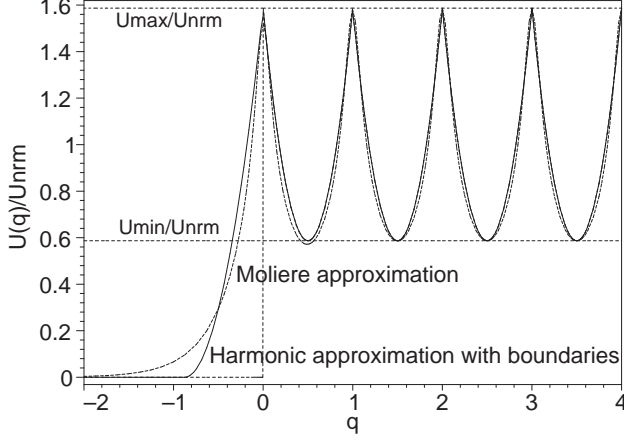


Fig. 2. The crystal potential for the range $\varphi_{min} < \varphi < \varphi_0$ in harmonic approximation with parameters $U_{max} = 35.9eV$, $U_{min} = 13.3eV$, and Moliere potential for Si (110) at T=300K. Notations: $q = (\rho - R_{min})/d_p$, $U_{nrm} = U_{max} - U_{min}$.

$$\begin{aligned} U_b * (\rho_b/d_p + 1/2)^2 &= U_{min}/2, \\ U_b * (\rho_b/d_p)^2 &= U_{max}, \end{aligned} \quad (4)$$

leads to the boundary semiparabolic potential with parameters:

$$\begin{aligned} U_b &= \frac{(2U_{max} - U_{min})^2}{U_{max} + U_{min}/2 + \sqrt{2U_{max}U_{min}}}, \\ \rho_b &= -d_p \frac{U_{max} + \sqrt{U_{max}U_{min}/2}}{2U_{max} - U_{min}}. \end{aligned} \quad (5)$$

Finally, the parabolic model of Moliere's potential (2) of the bent crystal with boundaries can be written (see Fig. 2)

$$U_0(\rho, \varphi) = \begin{cases} U_b \left(\frac{\rho - R_0 - \rho_b}{d_p} \right)^2, & \rho_b + R_0 < \rho < R_0, \varphi_{min} < \varphi < \varphi_0, \\ 0, & \text{otherwise,} \end{cases} \quad (6)$$

- for boundary and

$$U_n(\rho, \varphi) = \begin{cases} U_{nrm} \left(\frac{2(\rho - R_n - d_p/2)}{d_p} \right)^2 + U_{min}, & R_n < \rho < R_{n+1}, \\ & \varphi_{min} < \varphi < \varphi_n, \\ U_b \left(\frac{\rho - R_{n+1} - \rho_b}{d_p} \right)^2, & \rho_b + R_{n+1} < \rho < R_{n+1}, \\ & \varphi_n < \varphi < \varphi_{n+1}, \\ 0, & \text{otherwise,} \end{cases} \quad (7)$$

- for channels $0 \leq n \leq N - 1$. The boundary potential (6) does not play any role for bulk channeling, but may play an essential role for an aberration of the focusing, if the length of this potential along the n -th microbeam, $R_n(\varphi_{n+1} - \varphi_n)$, greater then the length of oscillation of particles inside the channel, $\lambda_c \cong d_p/\Psi_p$ (Ψ_p is the Lindhard critical angle for planar channeling). This condition may happen for extreme focusing with shortest focal length [12] (see also below) and a similar potential term at the end of each channel must be kept for corrections of phase curves (see second line of (7)). If this condition does not hold and distortion caused by boundaries is negligible, and the channel potential (6,7) becomes:

$$U_{b-c}(\rho, \varphi) = \sum_{n=0}^{N-1} U_n(\rho, \varphi), \quad (8)$$

where

$$U_n(\rho, \varphi) = \begin{cases} U_{nrm} \left(\frac{2(\rho - R_n - d_p/2)}{d_p} \right)^2 + U_{min}, & R_n < \rho < R_{n+1}, \\ & \varphi_{min} < \varphi < \varphi_n, \\ 0, & \text{otherwise.} \end{cases} \quad (9)$$

3 Dynamic of particles inside the bent crystal

Consider the motion of a relativistic spinless particles in potential (1) or (8). The Hamiltonian of the particle is defined by

$$H(Q, P) = c\sqrt{P_i P^i + m^2 c^2} + U_{b-c}(\rho, \varphi), \quad (10)$$

where $Q = \{\rho, \varphi\}$ and $P = \{p_\rho, p_\varphi\} = \{m\dot{\rho}\gamma, m\rho^2\dot{\varphi}\gamma\}$ are canonical coordinates and conjugate momenta of particle, $\gamma = (1 - (\dot{\rho}^2 + \rho^2\dot{\varphi}^2)/c^2)^{-1/2}$, $P_i P^i = p_\rho^2 + p_\varphi^2/\rho^2$. The Hamiltonian $H(Q, P)$ is a piecewise function of φ and ρ and, most important, does not depend on φ inside and outside of each individual channel. Hence, the angular momentum of particle $p_\varphi = m\rho^2\dot{\varphi}\gamma$ (see Fig. 1) is conserved inside and outside the crystal and may change only when particle crosses the boundaries of the crystal. The phase curves of the particles are described by system of Hamiltonian's equations ($\dot{P} = -\partial H(Q, P)/\partial Q$, $\dot{Q} = \partial H(Q, P)/\partial P$):

$$\dot{p}_\rho = \frac{cp_\varphi^2}{\rho^3\sqrt{P_i P^i + m^2 c^2}} - \partial U_{b-c}(\rho, \varphi)/\partial \rho, \quad \dot{p}_\varphi = 0,$$

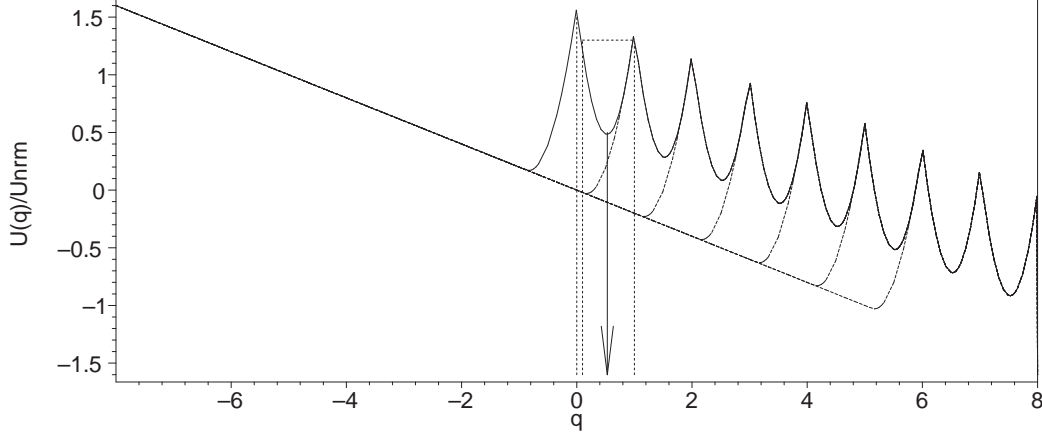


Fig. 3. The effective crystal potential for bounded crystal Si (110) at $T=300\text{K}$ in harmonic approximation, Eq. (6,7), for radial sections: $\varphi_{min} < \varphi < \varphi_0$ - solid line; $\varphi_0 < \varphi < \varphi_1$ and $\varphi_1 < \varphi < \varphi_2$ - dash lines. In the bent crystal, in addition to the normal channels, particle may also have a surface channel in which it moves sequentially reflecting from a surface plane. Note that this surface channel is much wider than the crystal channel and might play an important role for focusing in extreme conditions [12].

$$\dot{\rho} = \frac{cp_\rho}{\sqrt{P_i P^i + m^2 c^2}}, \quad \dot{\varphi} = \frac{cp_\varphi}{\rho^2 \sqrt{P_i P^i + m^2 c^2}}. \quad (11)$$

Using the fact, that last two equations of (11) can only be resolved if

$$\frac{c}{\sqrt{P_i P^i + m^2 c^2}} = \frac{1}{m\gamma}, \quad (12)$$

the system (11) can be written in the form:

$$\begin{aligned} \dot{p}_\rho &= \frac{p_\varphi^2}{m\gamma\rho^3} - \partial U_{b-c}(\rho, \varphi)/\partial\rho, & p_\varphi &= const, \\ \dot{\rho} &= \frac{p_\rho}{m\gamma}, & \dot{\varphi} &= \frac{p_\varphi}{\rho^2 m\gamma}. \end{aligned} \quad (13)$$

The Hamiltonian (10) of the system (13) has a cylindrical symmetry, therefore the angular momentum of the particle p_φ is conserved. The tangent momentum of particle p_φ/ρ along the curved channel is not exactly conserved, but taking into account that the channeling particle can not move further than $d_p/2$ from the center line of the channel and $d_p/R_n \ll 1$, the tangent momentum of particles $p_t = p_\varphi/\rho = m\rho\dot{\varphi}\gamma$ and tangent velocity $v_t = \rho\dot{\varphi} = p_t/(m\gamma)$ are conserved with high accuracy. We also make the following

approximations:

$$p_\rho \ll (p_t, mc),$$

$$\frac{p_\varphi^2}{m\gamma\rho^3} \simeq \frac{p_\varphi^2}{m\gamma R_{min}^3},$$

$$U_{b-c}(\rho, \varphi) \ll c\sqrt{P_i P^i + m^2 c^2}, \quad (14)$$

which mean that the incident particles are directed at the small angle to the crystalline planes, the centrifugal force $p_\varphi^2/(m\gamma\rho^3) = p_t v_t/\rho$ for all crystal channels is practically the same (the crystal thickness $d_c = Nd_p \ll R_{min}$), and gamma factor inside the crystal is changed by a small amount:

$$\gamma \simeq \gamma_o = \frac{\sqrt{p_{\rho o}^2 + p_{\varphi o}^2/\rho_o^2 + m^2 c^2}}{mc}, \quad (15)$$

From (11), (14) and (15) the well known equations [1] of motion of a particle in bent crystal can easily be received :

$$m\gamma_o \ddot{\rho} = \frac{p_\varphi^2}{m\gamma_o R_{min}^3} - \partial U_{b-c}(\rho, \varphi)/\partial \rho, \quad p_\varphi = const,$$

$$\dot{\rho} = \frac{p_\rho}{m\gamma_o}, \quad \dot{\varphi} = \frac{p_\varphi}{R_{min}^2 m\gamma_o}. \quad (16)$$

Note that parameter φ in Eq. (11,13,16) means only the piecewise character of potential (1, 8), which has discontinuity at the front and end surfaces of the each channel. The normal derivative of the potential $\partial U_{b-c}(\rho, \varphi)/\partial \varphi$ on these surfaces does not exist. Of course, the real atomic potential is smooth function on the surface. Its derivative rendering the normal force causes an impulse in normal linear momentum when the particles cross these surfaces. The linear momentum tangent to the front and end surfaces of the channels does not change as particle passes the boundary of the crystal, but angular momentum may slightly change due to force acting perpendicular to these surfaces. Thus, the boundary conditions for Eq.(11,13-16) on front surface of the crystal, $\varphi = \varphi_{min}$, can be presented in the form

$$\rho_o = \rho_i, \quad p_{\rho o} = p_{\rho i}, \quad p_{\varphi o} = p_{\varphi i} + \Delta p, \quad (17)$$

where $(\rho_o, p_{\rho o}, p_{\varphi o})$, $(\rho_i, p_{\rho i}, p_{\varphi i})$ denote the radial coordinate, linear tangent and angular momenta on the particle for $\varphi \rightarrow \varphi_{min}^-$ and $\varphi \rightarrow \varphi_{min}^+$ respectively. Using the law of conservation of the energy

$$c\sqrt{p_{\rho o}^2 + p_{\varphi o}^2/\rho_o^2 + m^2 c^2} = c\sqrt{p_{\rho i}^2 + p_{\varphi i}^2/\rho_i^2 + m^2 c^2} + U_{b-c}(\rho_i, \varphi_{min}), \quad (18)$$

we can receive a change in angular momentum p_φ in (17),

$$\Delta_p \cong \frac{\rho^2 \sqrt{p_{\rho o}^2 + p_{\varphi o}^2 / \rho_o^2 + m^2 c^2}}{c p_{\varphi o}} U_{b-c}(\rho_i, \varphi_{min}), \quad (19)$$

on the boundary of the crystal. The same boundary conditions (17) take place when the particle passes the end surface of the crystal. The assumption (14) allows also to split the energy of relativistic particles into kinetic energy of particle along the bent channel $E_{||}$ and transverse energy E_\perp [23,24,14,25,17]:

$$E \cong E_{||} + E_\perp, \quad (20)$$

$$E_\perp = \frac{p_\rho^2}{2m\gamma_o} + U_{b-c}(\rho, \varphi) - \frac{p_\varphi^2(\rho - R_{min})}{m\gamma_o R_{min}^3}, \quad E_{||} = c\sqrt{p_\varphi^2 / R_{min}^2 + m^2 c^2}.$$

The transverse energy E_\perp is constructed of three terms: the kinetic transverse energy, the static potential energy and centrifugal potential energy. The last two terms may be combined in one - the effective transverse potential in a bent crystal (see Fig. 3)):

$$U_{eff}(\rho, \varphi) = U_{b-c}(\rho, \varphi) - \frac{p_\varphi^2(\rho - R_{min})}{m\gamma_o R_{min}^3}. \quad (21)$$

Since the energy along the bent channel $E_{||}$ is conserved, the transverse energy E_\perp is also conserved. Equation (16) with the potential (8,9) and boundary conditions (17,19) can be easily resolved,

$$\begin{aligned} \rho &= (\rho_o - \rho_{c,n}) \cos(\omega t) + \frac{p_{\rho o}}{\omega m \gamma_o} \sin(\omega t) + \rho_{c,n}, \\ p_\rho &= p_{\rho o} \cos(\omega t) - (\rho_o - \rho_{c,n}) \omega m \gamma_o \sin(\omega t), \\ \varphi &= \Omega t + \varphi_{min}, \\ p_\varphi &= const, \end{aligned} \quad (22)$$

where the frequency of angular rotation, frequency of transverse oscillation and the radius of the central line of motion for n -channel are

$$\begin{aligned} \Omega &= \frac{p_\varphi}{m\gamma_o R_{min}^2}, \\ \omega &= \sqrt{\frac{8U_0}{m\gamma_o d_p^2}}, \\ \rho_{c,n} &= R_n + \frac{d_p}{2} + \frac{p_\varphi^2}{\omega^2 m^2 \gamma_o^2 R_{min}^3}. \end{aligned} \quad (23)$$

Thus, the motion of all particles in phase space can be described by Eqs. (22) with parameters (23). The maximum amplitude of oscillation and transverse momentum inside the bent crystal are (see Eq.(22) and Fig.3)

$$\begin{aligned} |\rho_{max} - \rho_{c,n}| &= \frac{d_p}{2} - \frac{p_\varphi^2}{\omega^2 m^2 \gamma_o^2 R_{min}^3}, \\ p_{\rho,max} &= \left(\frac{d_p}{2} - \frac{p_\varphi^2}{\omega^2 m^2 \gamma_o^2 R_{min}^3} \right) \omega m \gamma_o. \end{aligned} \quad (24)$$

To facilitate further calculations we introduce the normalized dimensionless local coordinates x, v_x for each channel:

$$x = \frac{\rho - \rho_{c,n}}{d_p/2}, \quad v_x = \frac{p_\rho}{\omega m \gamma_o d_p/2}, \quad (25)$$

which satisfy the equation of conservation transverse energy (20)

$$x^2 + v_x^2 = r_{ch}^2. \quad (26)$$

The parameter r_{ch} ,

$$\begin{aligned} r_{ch} &= 1 - \frac{2p_\varphi^2}{\omega^2 m^2 \gamma_o^2 R_{min}^3 d_p} = 1 - \frac{\epsilon}{\epsilon_c}, \\ \epsilon &= \frac{p_\varphi^2}{m \gamma_o R_{min}^3}, \quad \epsilon_c = \frac{4U_0}{d_p}, \end{aligned} \quad (27)$$

can be called the dimensionless radius of the microbeam in the phase space, and ϵ, ϵ_c are an effective electric field and critical electric field produced by bent crystal [4,3].

4 Statistical model of microbeam focusing

The classical approach to the kinetics of beams assumes the Boltzmann equation for particle distribution function $f = f(\vec{r}, \vec{p})$ in a steady state situation:

$$\vec{v} \frac{\partial f}{\partial \vec{r}} + e \vec{E} \frac{\partial f}{\partial \vec{p}} = St(f), \quad (28)$$

where $e\vec{E}$ is electric field acting upon the ion with charge e inside the crystal, $St(f)$ is a collision integral, which plays an important role in establishing the equilibrium states and dechanneling inside the crystal. Outside the crystal $St(f)$ and $e\vec{E}$ vanish and the Boltzmann equation reduces to particular simple form

$$\vec{v} \frac{\partial f}{\partial \vec{r}} = 0. \quad (29)$$

Consider 2-D geometry for plane channeling (Fig. (1a)). The particle beam has an initial distribution $f_{in}(x, z_{in}(x), v_x, v_z)$ on the entrance of the crystal surface $z = z_{in}(x)$ and some distribution $f_{out}(x, z_{out}(x), v_x, v_z)$ formed by channeling process on the end face of the crystal $z = z_{out}(x)$. We use Cartesian coordinate system instead of the cylindrical coordinates used in Sec.2,3 and assume that all coordinates and their conjugate momentums or velocities are dimensionless. Behind the crystal the Eq. (29) becomes

$$v_x \frac{\partial f(x, z, v_x, v_z)}{\partial x} + v_z \frac{\partial f(x, z, v_x, v_z)}{\partial z} = 0 \quad (30)$$

with general solution

$$f(x, z, v_x, v_z) = g(x - z * v_x/v_z, v_x, v_z), \quad (31)$$

where g is arbitrary function of three variables. The boundary condition on the end face of the crystal $z = z_{out}(x)$ gives unique solution for beam distribution ($v_z = const$):

$$g(x - z_{out}(x) * v_x/v_z, v_x, v_z) = f_{out}(x, z_{out}(x), v_x, v_z). \quad (32)$$

As a simple model, consider single channel, say channel with output angle φ_0 (see Fig.1a). Output particle distribution on the end face of the channel ($z_{out} = 0$) is

$$f_{out,0}(x, 0, v_x, v_z) = h(v_z) \begin{cases} \frac{1}{\pi r_{ch}^2}, & v_x^2 + x^2 < r_{ch}^2, \\ 0, & v_x^2 + x^2 \geq r_{ch}^2, \end{cases} \quad (33)$$

where $h(v_z)$ is some distribution in space of longitudinal component of the velocity, r_{ch} is the radius of particle distribution in the phase space which is

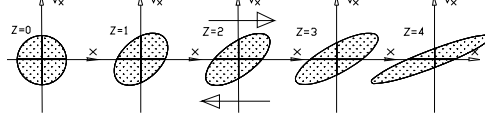


Fig. 4. Evolution of distribution function for microbeam from single channel. The trajectories of particle in 2D are parallel to the x axis. The phase profile along trajectories of particles moves with a constant velocity ($v_x = const$).

less than $d_p/2$ radius of crystal channel. The distribution (33) is normalized

$$\int_{-\frac{2}{d_p}}^{\frac{2}{d_p}} \int_{-\infty}^{\infty} \int_{-\infty}^{\infty} f_{out,0}(x, 0, v_x, v_z) dx dv_x dv_z = 1, \quad (34)$$

viz., one particle per one channel. By using boundary conditions (32) and (33) it is easy to show that the distribution function of this channel in phase space behind the crystal will be

$$f_{out,0}(x, z, v_x, v_z) = h(v_z) \begin{cases} \frac{1}{\pi r_{ch}^2}, & v_x^2 + (x - z \frac{v_x}{v_z})^2 < r_{ch}^2, \\ 0, & v_x^2 + (x - z \frac{v_x}{v_z})^2 \geq r_{ch}^2, \end{cases} \quad (35)$$

and the evolution of this distribution function along the axis z is shown in Fig.4. In phase space, the cross section of distribution is deformed, but the area of microbeam is conserved as well as the phase density along trajectories in the agreement with Liouville's theorem.

The same treatment can easily be extended to each channel if we take proper Cartesian coordinate system (\acute{x}, \acute{z}) with origin at the center of this channel on the end face of the crystal and with OX axis directed to the focus (see Fig.1b). The coordinate system for n channel is connected to Cartesian coordinates (x, z) of the 1st channel by following relations

$$\begin{aligned} x - x_n &= \acute{x}_n \cos(\vartheta_n) - \acute{z}_n \sin(\vartheta_n), \\ z - z_n &= \acute{x}_n \sin(\vartheta_n) + \acute{z}_n \cos(\vartheta_n), \end{aligned} \quad (36)$$

where the origins of (\acute{x}, \acute{z}) coordinate systems are

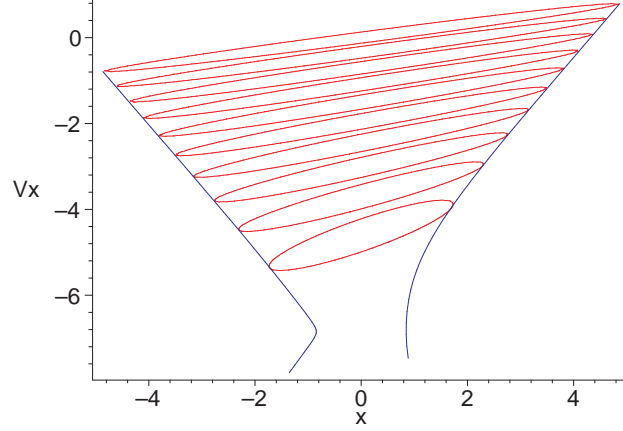


Fig. 5. The phase space of microbeams at focal spot when $F_{min} \ll F_{max}$. Only ten channels are taken for illustrative purposes. In fact, about 10^7 crystal (110) channels would typically be involve in forming a focal spot for the Si crystal with thickness $d_c = 2mm$.

$$\begin{aligned} x_n &= (R_{min} + nd_p + d_p/2)\cos(\vartheta_n) - R_{min}, \\ z_n &= (R_{min} + nd_p + d_p/2)\sin(\vartheta_n), \end{aligned} \quad (37)$$

and the angles $\vartheta_n = \varphi_n - \varphi_0$ defined by (see Fig.1a)

$$\sin(\vartheta_n) = \frac{(R_{min} + nd_p)\sqrt{D^2 - R_{min}^2} - R_{min}\sqrt{D^2 - (R_{min} + nd_p)^2}}{D^2}. \quad (38)$$

Among others important parameters of the focusing (Fig.1), there are simple formulas for the maximum and minimum focal distances

$$\begin{aligned} F_{max} &= \sqrt{D^2 - R_{min}^2}, \\ F_{min} &= \sqrt{D^2 - (R_{min} + d_c)^2}, \\ d_c &= Nd_p. \end{aligned} \quad (39)$$

The distribution function for n-th channel in phase space behind the crystal is

$$f_{out,n}(\dot{x}_n, \dot{z}_n, v_{\dot{x}_n}, v_{\dot{z}_n}) = h(v_{\dot{z}_n}) \begin{cases} \frac{1}{\pi r_{ch}^2}, & v_{\dot{x}_n}^2 + (\dot{x}_n - \dot{z}_n \frac{v_{\dot{x}_n}}{v_{\dot{z}_n}})^2 < r_{ch}^2, \\ 0, & v_{\dot{x}_n}^2 + (\dot{x}_n - \dot{z}_n \frac{v_{\dot{x}_n}}{v_{\dot{z}_n}})^2 \geq r_{ch}^2, \end{cases} \quad (40)$$

The equations (36) represent a reversible transformation, i.e. that they also define the (\dot{x}_n, \dot{z}_n) as functions of the (x, z) , or, in other words, that they are soluble with respect to the (\dot{x}_n, \dot{z}_n)

$$\begin{aligned} \dot{x}_n &= (x - x_n)\cos(\vartheta_n) + (z - z_n)\sin(\vartheta_n), \\ \dot{z}_n &= -(x - x_n)\sin(\vartheta_n) + (z - z_n)\cos(\vartheta_n). \end{aligned} \quad (41)$$

For the distribution function (35) we have also to calculate $v_{\dot{x}_n}$ and $v_{\dot{z}_n}$ which can be done by differentiating (41) with respect to t :

$$\begin{aligned} v_{\dot{x}_n} &= v_x\cos(\vartheta_n) + v_z\sin(\vartheta_n), \\ v_{\dot{z}_n} &= -v_x\sin(\vartheta_n) + v_z\cos(\vartheta_n). \end{aligned} \quad (42)$$

Note that the distribution in longitudinal space of the velocities is invariant under the changes of (42), i.e. $h(v_z) = h(v_{\dot{z}_n})$. Substituting in the equation (40) the values of the $(\dot{x}_n, \dot{z}_n, v_{\dot{x}_n}, v_{\dot{z}_n})$ given by formulas (41), (42), we get the equation for distribution functions for all channels in coordinates (x, z, v_x, v_z)

$$f_{out,n}(x, z, v_x, v_z) = h(v_z) \begin{cases} \frac{1}{\pi r_{ch}^2}, & (v_x\cos(\vartheta_n) + v_z\sin(\vartheta_n))^2 + \\ & \left((x - x_n)\cos(\vartheta_n) + (z - z_n)\sin(\vartheta_n) - \right. \\ & \left. ((x - x_n)\sin(\vartheta_n) - (z - z_n)\cos(\vartheta_n)) \right. \\ & \left. \frac{v_x\cos(\vartheta_n) + v_z\sin(\vartheta_n)}{v_x\sin(\vartheta_n) - v_z\cos(\vartheta_n)} \right)^2 < r_{ch}^2, \\ 0, & (v_x\cos(\vartheta_n) + v_z\sin(\vartheta_n))^2 + \\ & \left((x - x_n)\cos(\vartheta_n) + (z - z_n)\sin(\vartheta_n) - \right. \\ & \left. ((x - x_n)\sin(\vartheta_n) - (z - z_n)\cos(\vartheta_n)) \right. \\ & \left. \frac{v_x\cos(\vartheta_n) + v_z\sin(\vartheta_n)}{v_x\sin(\vartheta_n) - v_z\cos(\vartheta_n)} \right)^2 \geq r_{ch}^2, \end{cases} \quad (43)$$

The final distribution function for the beam behind the crystal is

$$f_{out}(x, z, v_x, v_z) = \sum_{n=0}^{N-1} f_{out,n}(x, z, v_x, v_z), \quad (44)$$

where $N = d_c/d_p$ - number of plane channels of crystal. If we substitute $z = F_{max}$ in (44), we can get the distribution function in a focal plane of the phase space. The main features of this distribution can be seen in Fig.5. All ellipse have the same area as mentioned above. The upper ellipse is shaped by microbeam from channel 0. It has greater x-size because the larger distance from the output channel to the focal point. The bottom ellipse is related to

the last microbeam. It has a smallest deformation. The centers of the ellipses in focal plane are located on the V_x -axis at the points

$$v_{x,n} = -\frac{v_z \sin(\vartheta_n)}{\cos(\vartheta_n)}. \quad (45)$$

For an experiment measurements, it is important to find the intensity profile at the focal spot. It can be received by the integrating Eq.(44) over v_x :

$$f_{out}(x, F_{max}) = \int \int \sum_{n=0}^{N-1} f_{out,n}(x, F_{max}, v_x, v_z) dv_x dv_z. \quad (46)$$

In practical calculations, the summation over a pile of channels (see Fig.5) can be change by integrating over n . To simplify the calculations, we assume that all $\vartheta_n \ll 1$. For normalization (34) this gives the pick value of distribution function in the form

$$\begin{aligned} f_{out}(0, F_{max}) = & 2 r_{ch} v_z \left(\frac{\sqrt{v_z^2 + D^2 \cos(\Gamma)^2}}{D d_p \sin(\Gamma)} - \right. \\ & \left. - \frac{v_z^2 + D^2 \cos(\Gamma)^2}{D d_p \sin(\Gamma) \sqrt{v_z^2 + D^2 \cos(\Gamma)^2 - 2 D d_p \sin(\Gamma) N}} \right) + \\ & + 4 \frac{r_{ch} v_z N}{\sqrt{v_z^2 + D^2 \cos(\Gamma)^2 - 2 D d_p \sin(\Gamma) N}}, \end{aligned} \quad (47)$$

where the following parameters were introduced

$$\begin{aligned} \sin(\Gamma) &= \frac{R_{min}}{D}, \\ \cos(\Gamma) &= \frac{\sqrt{D^2 - R_{min}^2}}{D}. \end{aligned} \quad (48)$$

Note that in order to calculate the envelope of the beam in phase space, we may take a derivative of microbeam surface with respect to n considering variable n as continuous and eliminate n from two equations

$$\begin{aligned} \Phi_n(x, z, v_x, v_z) &= 0, \\ \frac{\partial \Phi_n(x, z, v_x, v_z)}{\partial n} &= 0, \end{aligned} \quad (49)$$

where $\Phi_n(x, z, v_x, v_z) = 0$ is the equation of the microbeam surface in phase space. We can substitute z for F_{max} (see Eq.(39)) in equations (49), so getting

$$\begin{aligned}\Phi_n(x, F_{max}, v_x, v_z) &= 0, \\ \frac{\partial \Phi_n(x, F_{max}, v_x, v_z)}{\partial n} &= 0,\end{aligned}\tag{50}$$

the equations of the cross section envelope line at the focal spot. If the distribution (40) or (43) is used as a model, we have the implicit equation of n-th microbeam in focal plane (x, v_x) which actually used to depict Fig.5:

$$\Phi_n(x, F_{max}, v_x, v_z) = \frac{(Bv_s - Cx)^2}{(v_s \sin(\vartheta_n) - C)^2} + v_s^2 - \frac{r_{ch}^2}{1 - \sin(\vartheta_n)^2} = 0.\tag{51}$$

The coefficients B, C here are given functions of the ϑ_n :

$$\begin{aligned}C &= \frac{v_z}{\sqrt{1 - \sin(\vartheta_n)^2}}, \\ B &= D \cos(\Gamma + \vartheta_n), \\ v_s &= v_x + C \sin(\vartheta_n)\end{aligned}\tag{52}$$

The calculation of the envelope by Eq.(50) with surface (51) are straightforward but cumbersome. In the case $v_s \sin(\vartheta_n) \ll C$, which is always true for fast particles, the envelope has a form of two deformed hyperbolas with asymmetry. The parametric presentation for these curves $(x_1, v_{x,1}), (x_2, v_{x,2})$ are (the parameter for curves is ϑ_n)

$$\begin{cases} x_1 = \frac{r_{ch} \sqrt{B^2 + C^2}}{C \cos(\vartheta_n)} \\ v_{x,1} = \frac{r_{ch} B}{\sqrt{B^2 + C^2} \cos(\vartheta_n)} - C \sin(\vartheta_n) \end{cases}, \quad \begin{cases} x_2 = -\frac{r_{ch} \sqrt{B^2 + C^2}}{C \cos(\vartheta_n)} \\ v_{x,2} = -\frac{r_{ch} B}{\sqrt{B^2 + C^2} \cos(\vartheta_n)} - C \sin(\vartheta_n) \end{cases},\tag{53}$$

where $B = B(\vartheta_n), C = C(\vartheta_n)$ are defined in Eqs.(52). These formulas are accurate for foci located far away from the crystal as well as for crystalline geometry provided the maximum magnification and minimum focusing size proposed in [12]. The envelope calculated from them is shown in Fig. 5.

5 Conclusion

In conclusion, we describe some possible limitations of focusing which can substantially reduce the focusing effect. The smoothness of the cylindrical surface is of great importance, the amorphous layer on that surface must be as thin as possible, and all adjacent channels must constitute the staircase with step widths equals to the interplaner space. Of course, it is not always possible and deviation caused by surface roughness or mosaic blocks with widths about the length of channeling oscillation will produce a broadening of the focal spot and greatly decrease the peak intensity. Other well known source of aberration to be considered for focusing is negative Gaussian curvature of bent crystals (anticlastic effect). The asymmetry of centripetal dechanneling in bent channels [3,4] is a strong source of asymmetry in focal spot. There is also a possibility of asymmetry in coherent transitional scattering when the particles come out with small angles and move some short period of time in semichannel. For long crystal, dechanneling plays an important role, and the maximum possible focal distance [12] when the focal spot lies almost on the tip of the crystal is limited by this process.

References

- [1] E. N. Tsyganov, Some aspects of the mechanism of a charge particle penetration through a monocrystal, Fermilab, TM-682 (1976) 5.
- [2] R. A. Carrigan, Developments in relativistic channeling, in: S. Chattopadhyay, J. McCullough, P. Dahl (Eds.), *Advanced Accelerator Concepts*. Plenum, New York, 1997, pp. 146–163.
- [3] V. M. Biryukov, Y. A. Chesnokov, V. I. Kotov, *Crystal Channeling and Its Application at High-Energy Accelerators*, Springer, Verlag Berlin Heidelberg, 1997.
- [4] A. M. Taratin, Particle channeling in a bent crystal, *Phys. Particles Nuclei* 29 (5) (1998) 437–462.
- [5] Y. N. Adishchev, et al., *JETP lett.* 30 (1979) 402.
- [6] R. A. Carrigan, On the possible applications of the steering of charged particles by bent single crystal, Fermilab FN-80/45 (1980) 46.
- [7] R. A. Carrigan, The application of channeling in bent crystals to charged particle beams, in: R. A. Carrigan, J. A. Ellison (Eds.), *Relativistic Channeling*. Plenum, New York, 1987, pp. 339–368.
- [8] C. R. Sun, Application of channeling to particle physics, in: R. A. Carrigan, J. A. Ellison (Eds.), *Relativistic Channeling*. Plenum, New York, 1987, pp. 379–397.

- [9] A. Schafer, W. Greiner, Possible use of mixed crystals to focus ion beam, J. Phys. G: Nulc. Part. Phys. 17 (1991) L217–L221.
- [10] A. S. Denisov, O. L. Fedin, M. A. Gordeeva, et al., First results from study of a 70 gev proton beam being focused by bent crystal, Nucl. Instr. and Meth. B 69 (1992) 382–384.
- [11] V. I. Baranov, et al., Results of studying 70gev proton beam focusing by bent crystal, in: XVth International Conference on High Energy Accelerators, Hamburg, Germany, July 20-24, 1992, pp. 128–130.
- [12] G. V. Kovalev, Focusing limits of high energy particles in bent crystal, Nucl. Inst. and Meth. B 207 (2003) 482–486.
- [13] J. Lindhard, Influence of crystal lattice on motion of energetic charged particles, Danske Vid. Selsk. Mat.-Fys. Medd. 34 (1965) no.14.
- [14] A. M. Taratin, Y. M. Filimonov, E. G. Vyatkin, S. A. Vorobiev, Phys. Status Solidi B 100 (1980) 273.
- [15] H. Kudo, Nucl. Instr. and Meth. 189 (1981) 609.
- [16] J. A. Ellison, Bending of gev particle beams by channeling in bent crystal planes, Nuclear Phys. B206 (1) (1982) 205–220.
- [17] J. A. Ellison, The theory of particle motion in straight and distorted crystals, in: R. A. Carrigan, J. A. Ellison (Eds.), Relativistic Channeling. Plenum, New York, 1987, pp. 79–88.
- [18] G. Moliere, Theorie der steuung schneller geladener teilhen 1, Z. Naturforsch 2A (1947) 133–145.
- [19] B. R. Appleton, C. Erginsoy, W. M. Gibson, Phys. Rev. 161 (1967) 330.
- [20] D. S. Gemmell, Channeling and related effects in the motion of charged particles through crystals, Rev. Mod. Phys. 46 (1) (1974) 129–227.
- [21] J. C. Poizat, Remillieux, Phys. Rev. Lett 27 (1971) 6.
- [22] J. H. Barrett, Phys. Rev. B3 (1971) 1527.
- [23] A. P. Pathak, Phys. Rev. B13 (1976) 4648.
- [24] V. V. Kaplin, S. A. Vorob'ev, Sov.Tech.Phys.Lett. 4 (1978) 78.
- [25] A. M. Taratin, S. A. Vorobiev, Phys. Status Solidi B 107 (1981) 521.